Probing Dielectric Breakdown in Single Crystal Hexagonal Boron Nitride

Citation for the original published paper (version of record):
Ranjan, A., Yankovich, A., Watanabe, K. et al (2023). Probing Dielectric Breakdown in Single Crystal Hexagonal Boron Nitride. Microscopy and Microanalysis, 29(1): 1998-2000. http://dx.doi.org/10.1093/micmic/ozad067.1034

Probing Dielectric Breakdown in Single Crystal Hexagonal Boron Nitride

Alok Ranjan, Andrew B Yankovich, Kenji Watanabe, Takashi Taniguchi, Eva Olsson

Microscopy and Microanalysis, **29** (Suppl 1), 2023, 1998–2000
https://doi.org/10.1093/micmic/ozad067.1034

Microscopy AND Microanalysis

Meeting-report

Probing Dielectric Breakdown in Single Crystal Hexagonal Boron Nitride

Alok Ranjan[1,*], Andrew B. Yankovich[1], Kenji Watanabe[2], Takashi Taniguchi[2], and Eva Olsson[1,*]

[1]*Department of Physics, Chalmers University of Technology, Gothenburg, Sweden*
[2]*National Institute of Materials Science, Tsukuba, Japan*

*Corresponding authors: alok.ranjan@chalmers.se, eva.olsson@chalmers.se

Hexagonal boron nitride (h-BN) is a 2D crystalline wide bandgap (~ 6 eV) material in with each layer is connected by van der Walls forces [1]. h-BN has a hexagonal lattice, akin to graphene, and its atomically flat and defect-free surface makes it a promising substrate for 2D semiconductors [2]. h-BN has shown promising applications in numerous emerging technologies including sensing, quantum cryptography and nano-electronics beyond silicon [3]. h-BN is widely used as a gate dielectric in transistors and a switching material in resistive switching devices [4, 5]. Prior works have studied the charge transport [4, 6], random telegraph noise [7] and breakdown field strength [4, 6-9], and have proposed the breakdown mechanism in h-BN [10, 11]. Electrical measurements have shown that defects are progressively generated in h-BN under electrical stress and upon accumulation of defects with formation of nanoscale defective regions, a dielectric breakdown is triggered [12]. The regions drive very high current leading to the failure of a transistor. In many instances, these nanoscale conduction filaments (CFs) can be dissolved upon application of electrical stress with reverse polarity, allowing the device to recover its conductivity, and hence used in emerging non-volatile resistive switching applications [5]. The physical and chemical nature of these CFs is still debated and, hence, it is crucial to gain further insights about their structure and chemical composition. As typical device dimensions are few micrometers, it is challenging to reliably locate these randomly generated nanoscale CFs, and this is the motivation for our work where we aim to locate the CFs.

We have fabricated Au (bottom electrode)/h-BN/Ag (top electrode) nanocapacitors, as shown in Fig. 1a. h-BN is monocrystalline, and the area of the tested capacitor is 500 nm × 500 nm, as shown by the optical micrograph in the inset of Fig. 1b. The thickness of the h-BN flake is 6 nm and the separation between each capacitor is 500 nm. The capacitors are electrically stressed using a modified conduction atomic force microscope (CAFM) in which an electrical bias is applied to the CAFM tip, and the bottom Au electrode is grounded [12]. The breakdown field (ξ_{BD}) of the fabricated capacitors is measured to be ~12 MV/cm. We use fields of $\xi = 7.5$ MV/cm for stress testing because this is lower than the ξ_{BD}, allowing us to monitor the evolution of current with time, as shown in Fig. 1b. These measurements are known as time dependent dielectric breakdown (TDDB) tests and are commonly used to study the reliability of gate dielectrics [13]. Multiple jumps in current are observed before the current reaches the level of 500 nA (see inset of Fig. 1a), suggesting the formation of multiple CFs [14]. After electrical stressing, a FEI Versa 3D FIB-SEM is used to prepare cross-sectional transmission electron microscopy (TEM) samples. A key advantage of our experimental approach is that multiple stressed capacitors can be included in a single TEM lamella which greatly improves the yield of sample fabrication to capture these CFs. Scanning TEM (STEM) measurements are carried out at 200 kV on a JEOL Mono NEOARM 200F instrument equipped with a monochromator, an imaging and probe aberration corrector, a Gatan Imaging Filter continuum HR electron energy loss spectrometer (EELS) and an energy dispersive X-ray spectrometer (EDS).

The annular dark field (ADF) STEM micrograph shown in Fig. 2a displays a clear change in the contrast within the h-BN layer inside the stressed capacitor area. EELS maps of B and N in the region highlighted by the dashed white square in Fig. 2a are shown in Figures 2b,c. EDS maps for Ag and Au obtained from the same region are shown in Figures 2d,e. Line profiles in the middle of h-BN layer throughout the capacitor area are shown in Fig. 2f. Here, the line profile has been obtained by integrating 5 pixels along the normal directions to the h-BN layer (corresponding to a width of 2.5 nm h-BN) to show the average trends. We observe a global reduction of B and N as well as an associated increase in Ag and Au signals within the stressed h-BN regions. Further analysis of the stressed capacitor shows the formation of multiple nanoscale CFs as shown by the representative STEM micrograph in Fig. 3a. The CF is conical in shape and has a width of ~20 nm to form a bridge connecting the top Ag and the bottom Au electrodes. EELS and EDS elemental analysis in Figures 3b-f shows that the CF predominantly consists of Ag and Au. Our work provides an experimental platform to probe and study single CFs using STEM imaging, diffraction, and spectroscopy. This work may be relevant for the study of dielectric breakdown and resistive switching phenomenon in emerging materials [15].

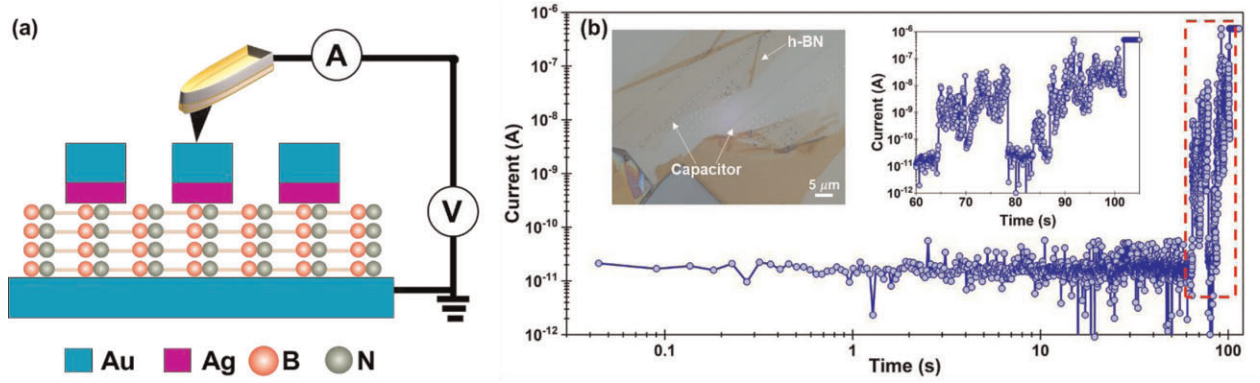

Fig. 1. (a) Schematic diagram showing a cross-sectional view of a Au/h-BN/Ag capacitor and the electrical connections for the CAFM measurements. (b) TDDB characteristics measured on a 500 nm × 500 nm capacitor showing the evolution of leakage current with time. The applied electrical field is 7.5 MV/cm. The inset image shows an optical micrograph of the fabricated capacitor.

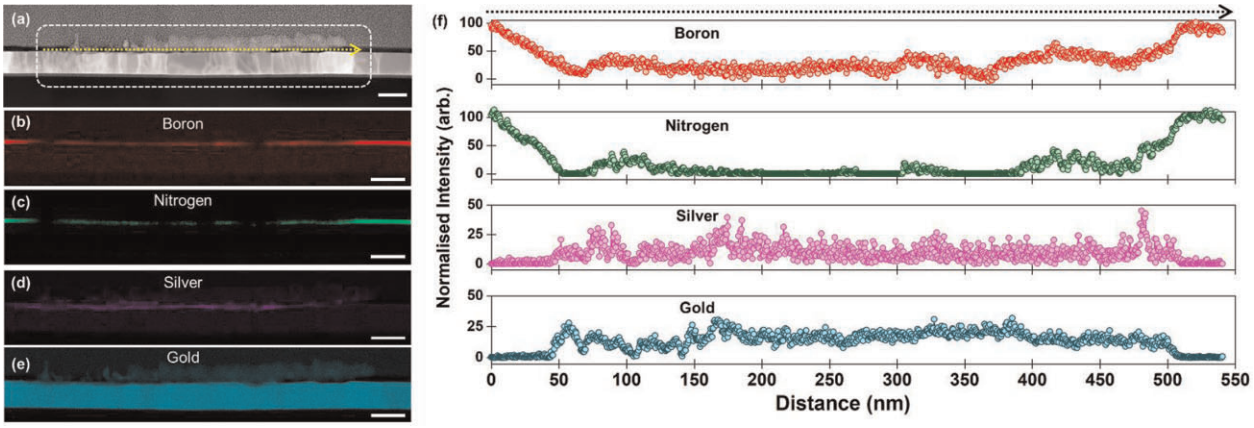

Fig. 2. (a) ADF STEM micrograph showing the cross-sectional view of the capacitor measured in Fig. 1(b) after electrical stress. (b, c) EELS maps showing the elemental distribution of B and N. (d, e) EDS maps showing the distribution of Ag and Au. Scale bars in (a) - (e) are 50 nm. (f) Line profiles across h-BN layer in the capacitor showing the distribution of B, N, Ag and Au. Note the significant increase in Ag and Au within the h-BN layer throughout the capacitor area.

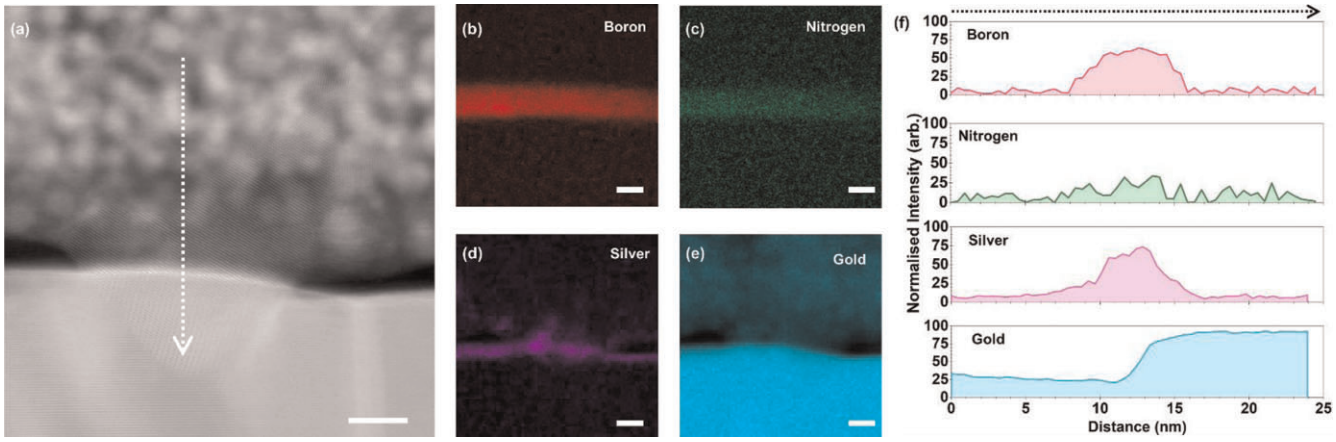

Fig. 3. (a) ADF STEM micrograph showing a conical conductive filament. The filament forms a bridge connecting the top Ag and the bottom Au electrode. (b, c) EELS maps showing the distribution of B and N. (d, e) EDS maps showing the distribution of Ag and Au. The scale bars in (a) – (e) are 5 nm. (f) Line profiles of B, N, Ag and Au across the white line shown in (a) revealing the CF is predominantly composed of Ag and Au.

References

1. K Watanabe *et al.*, *Nature Materials* **3** (2004), p. 404.
2. CR Dean *et al.*, *Nature Nanotechnology* **5** (2010), p. 722.
3. S Roy *et al.*, *Advanced Materials* **33**(44) (2021), p. 2101589.
4. L Britnell *et al.*, *Nano Letters* **12**(3) (2012), p. 1707.
5. Y Shi *et al.*, *Nature Electronics* **1**(8) (2018), p. 458.

6. U Chandni *et al.*, *Nano Letters* **15**(11) (2015), p. 7329.
7. A Ranjan *et al.*, *Applied Physics Letters* **112**(13) (2018), p. 133505.
8. Y Hattori *et al.*, *ACS Applied Material and Interfaces* **8**(41) (2016), p. 27877.
9. GH Lee *et al.*, *Applied Physics Letters* **99**(24) (2011), p. 243114.
10. Y Hattori *et al.*, *ACS Nano* **9**(1) (2015), p. 916.
11. A Ranjan *et al.*, *IEEE International Reliability Physics Symposium*, (2018), p. 4A1.
12. A Ranjan *et al.*, ACS Applied Material and Interfaces, Published, (2023).
13. EY Wu, *IEEE Transactions on Electron Devices* **66**(11) (2019), p. 4523.
14. EY Wu and J Sune, *IEEE Electron Device Letters* **24**(11) (2003), p. 692.
15. We acknowledge funding from the 2DTech Vinnova Competence Centre at Chalmers University of Technology. A. Ranjan acknowledges the travel grant from Chalmerska forskningsfonden. This work was performed in part at Myfab Chalmers and Chalmers Material Analysis Laboratory (CMAL). A. Ranjan greatly appreciates assistance of Sean O'Shea in the conduction AFM measurements.